ACADEMIC PRESS

Available online at www.sciencedirect.com

SCIENCE DIRECT®

Journal of Sound and Vibration 263 (2003) 709–724

JOURNAL OF SOUND AND VIBRATION

www.elsevier.com/locate/jsvi

H_2 active vibration control for offshore platform subjected to wave loading

Hua Jun Li[a,*], Sau-Lon James Hu[b], Christopher Jakubiak[b]

[a] *College of Engineering, Ocean University of Qingdao, Qingdao 266071, China*
[b] *Department of Ocean Engineering, University of Rhode Island, Narragansett, RI 02882, USA*

Received 14 September 2001; accepted 8 July 2002

Abstract

Offshore platforms are usually located in hostile environments. These platforms undergo excessive vibrations due to wave loads for both normal operating and extreme conditions. To ensure safety, the displacements of the platforms need to be limited, whereas for the comfort of people who work at the structures, accelerations also need to be restricted. This article is devoted to developing a proper procedure on applying H_2 control algorithm for controlling the lateral vibration of a jacket-type offshore platform by using an active mass damper. In comparison with earlier studies, a number of improvements in problem formulation, wave force filter design, and control algorithm implementation are made. The present paper also numerically demonstrated the effectiveness of H_2 active control. As expected, it significantly outperforms the corresponding passive control that uses a tuned mass damper.

1. Introduction

The history of structural designs can be roughly divided into three eras: classical, modern, and post-modern. Much of the classical era for civil structural designs dealt only with static loads. The modern era of structural design added specifications on the dynamic response. Today, major civil infrastructures must be designed to satisfy both static and dynamic requirements in the presence of a specified class of external loads. The post-modern era anticipates specifications on the dynamic response in some cases that are so severe that they can only be met by feedback control [1,2].

*Corresponding author.
E-mail address: lihuaj@public.qd.sd.cn (H.J. Li).

0022-460X/03/$ - see front matter
PII: S0022-460X(02)01095-7

In literature, extensive studies about feedback control have been conducted theoretically and experimentally. Housner et al. [2] reviewed the state-of-the-art in structural vibration control for civil engineering applications and cited over 300 articles. Among those studies, different kinds of control devices, control algorithms and external loads (e.g. wind and earthquake loads) were considered for bridges and high-rise buildings. Only a handful of studies were devoted to active control for offshore structures subjected to waves [3–5]. As stated in Suhardjo and Kareem [6], the active structural vibration control for offshore structures has not been appropriately investigated.

Dynamic loadings such as earthquake, wind and wave are usually modelled as stochastic processes characterized in the frequency domain by power spectral density functions. Frequency domain optimal control strategies allow the designer to directly deal with these natural representations of the excitation during control design. The frequency domain approaches also offer other attractive features, including that they allow the designer to specify disturbance attenuation over a desired frequency range, as well as roll-off the control action at high frequency. One of the frequency domain methods for controller design which has received much attention is H_2 control. Spencer et al. [7] was the first to apply H_2 control strategies to civil engineering structures for seismic protection purposes. Suhardjo and Kareem [6] extended the application of H_2 control algorithm to a jacket-type offshore platform in which the platform was modelled as a shear building. Due to the mathematical requirement of H_2 control algorithm that the input must be white noise processes, both studies utilized a force filter to produce intended environmental loading, i.e., passing a white noise process through the force filter to produce the intended loading characteristics. However, they failed to include additional white noise terms to account for the uncertainties associated with dynamic models. One intention of this article is to specify a right way of applying H_2 control algorithm to civil structures subjected to non-white excitations. Furthermore, in comparison with the study by Shuardjo and Kareem [6], this study also makes a number of improvements related to the problem formulation and methodology for applying H_2 control algorithm to a jacket-type offshore platform. In particular, a new and efficient approach on the wave force filter design is presented.

2. Preliminaries

The use of frequency domain analysis for a system is often more efficient than the time domain analysis if the analysis is to be done over an extended period of time. Large time histories of loading and response can be very cumbersome to work with, whereas a frequency domain analysis can solve for any length of time all at once. This method is especially useful in the problem of an offshore structure subject to a spectral wave loading which is already expressed in the frequency domain. Frequency domain descriptions of linear time-invariant systems are useful in analysis of the stability and response. The modal properties are expressed directly in system *transfer functions*, and the computationally difficult convolution integrals are replaced by equivalent multiplications of transforms and transfer functions in the frequency domain.

A linear constant continuous-time system is represented by either a transfer function, or its state space description. Let the continuous-time system be written in the state space form:

$$\dot{\mathbf{x}}(t) = \mathbf{A}\mathbf{x}(t) + \mathbf{B}\mathbf{u}(t) \tag{1}$$

and

$$\mathbf{y}(t) = \mathbf{C}\mathrm{x}(t) + \mathbf{D}\mathbf{u}(t), \tag{2}$$

where $\mathbf{x}$ is the state variable vector, $\mathbf{u}$, $\mathbf{y}$ the input and output vector, respectively, $\mathbf{A}$, $\mathbf{B}$, $\mathbf{C}$, $\mathbf{D}$ the matrices of proper dimensions, and the dot over a symbol indicates taking derivative with respect to time, t. Taking Laplace transform of Eqs. (1) and (2) yields the corresponding s-domain description as (assuming initial conditions $\mathbf{x} = 0$)

$$s\mathbf{x}(s) = \mathbf{A}\mathbf{x}(s) + \mathbf{B}\mathbf{u}(s) \tag{3}$$

and

$$\mathbf{y}(s) = \mathbf{C}\mathbf{x}(s) + \mathbf{D}\mathbf{u}(s), \tag{4}$$

where s is the complex Laplace variable. From Eq. (3), one obtains

$$\mathbf{x}(s) = (s\mathbf{I} - \mathbf{A})^{-1}\mathbf{B}\mathbf{u}(s) \tag{5}$$

then from Eq. (4)

$$\mathbf{y}(s) = [\mathbf{C}(s\mathbf{I} - \mathbf{A})^{-1}\mathbf{B} + \mathbf{D}]\mathbf{u}(s), \tag{6}$$

where $\mathbf{I}$ is the identity matrix. The *transfer function matrix* from $\mathbf{u}$ to $\mathbf{y}$, denoted as $\mathbf{T}_{\mathbf{yu}}(s)$, thus can be written as

$$\mathbf{T}_{\mathbf{yu}}(s) = \frac{\mathbf{y}(s)}{\mathbf{u}(s)} = \mathbf{C}(s\mathbf{I} - \mathbf{A})^{-1}\mathbf{B} + \mathbf{D}. \tag{7}$$

The above relationship can be described in a block diagram as shown in Fig. 1. It is noted that $\mathbf{T}_{\mathbf{yu}}(s)$ is completely defined by the constant matrices: $\mathbf{A}, \mathbf{B}, \mathbf{C}$ and $\mathbf{D}$. A conventional way to represent the $\mathbf{T}_{\mathbf{yu}}(s)$ is written as

$$\mathbf{T}_{\mathbf{yu}} := \begin{bmatrix} \mathbf{A} & \mathbf{B} \\ \mathbf{C} & \mathbf{D} \end{bmatrix}. \tag{8}$$

Using a general block diagram description, the H_2 control problem can be depicted as in Fig. 2. In this figure, $\mathbf{P}$ represents the plant transfer function and $\mathbf{K}$ the controller transfer function. The vector valued signals, $\mathbf{d}$, $\mathbf{u}$, $\mathbf{z}$ and $\mathbf{y}$ represent the following: $\mathbf{d}$ is the exogenous signals representing disturbances, sensor noise, model uncertainty, etc., $\mathbf{u}$ is the control signal, $\mathbf{z}$ is the signal of the regulated output; and $\mathbf{y}$ is the measured signal. The regulated output vector $\mathbf{z}$ may consist of any combination of states of the system and components of the control input vector $\mathbf{u}$. By appropriate choice of elements of $\mathbf{z}$, different control design objectives can be included in the problem

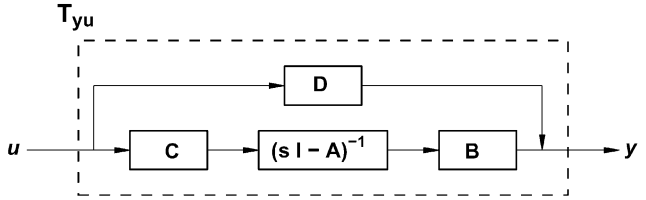

Fig. 1. Block diagram for $\mathbf{T}_{\mathbf{yu}}(s)$.

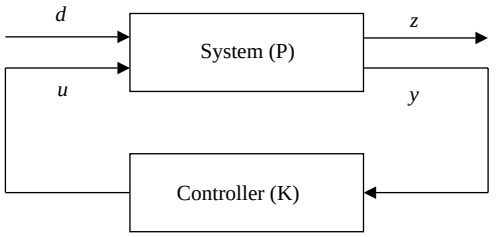

Fig. 2. Closed-loop control system configuration.

formulation. Weighting functions can be added to elements of **z** to determine the frequency range where each element of **z** is to be minimized. The "generalized" plant **P** in Fig. 2 can then contain the structure plus filters and weighting functions in frequency domain. The H_2 optimal control problem consists in finding an optimal compensator **K** that internally stabilizes **P** and minimizes the H_2 norm of the closed-loop transfer function matrix from **d** to **z**, that is, $\|\mathbf{T_{ZD}}\|_2$. The optimal controller **K** is constrained to provide *internal stability* which means that the states of **P** and **K** go to zero from all initial values when $\mathbf{d} = \mathbf{0}$. The H_2 norm of a stable transfer function matrix $\mathbf{T_{zd}}$ is defined as [8,9]

$$\|\mathbf{T_{zd}}\|_2 = \sqrt{tr\left\{\frac{1}{2\pi}\int_{-\infty}^{\infty} \mathbf{T_{zd}}(\mathrm{j}\omega)\mathbf{T_{zd}^*}(\mathrm{j}\omega)\,\mathrm{d}\omega\right\}}, \tag{9}$$

where *tr* stands for the trace of a matrix, $\mathrm{j} = \sqrt{-1}$ and $\mathbf{T_{zd}}^*$ is the complex conjugate transpose of $\mathbf{T_{zd}}$. More physical insight into the meaning of the H_2 norm can be obtained by noting that the H_2 norm of a transfer function measures the r.m.s. (root mean square) value of its output in a vector case, when the input is a *unit white noise* excitation vector. The r.m.s. value of the output vector **z** is defined as

$$\|\mathbf{z}\|_{\mathrm{r.m.s.}} = \sqrt{\sum_{i=1}^{n} E[z_i^2(t)]}, \tag{10}$$

where $E[\cdot]$ is the expected value operator, z_i is the ith component of **z**, and n is the number of components for the output vector **z**.

In Fig. 2, to obtain the transfer function $\mathbf{T_{zd}}$, partitioning P into its components, i.e.,

$$\mathbf{P} = \begin{bmatrix} \mathbf{P_{zd}} & \mathbf{P_{zu}} \\ \mathbf{P_{yd}} & \mathbf{P_{yu}} \end{bmatrix}. \tag{11}$$

It follows

$$\mathbf{z} = \mathbf{P_{zd}}\mathbf{d} + \mathbf{P_{zu}}\mathbf{u}, \quad \mathbf{y} = \mathbf{P_{yd}}\mathbf{d} + \mathbf{P_{yu}}\mathbf{u}, \quad \mathbf{u} = \mathbf{K}\mathbf{y}. \tag{12}$$

From the above relationships, the overall transfer function matrix from **d** to **z** for the closed-loop system can then be written as [10]

$$\mathbf{T_{zd}} = \mathbf{P_{zd}} + \mathbf{P_{zu}}\mathbf{K}(\mathbf{I} - \mathbf{P_{yu}}\mathbf{K})^{-1}\mathbf{P_{yd}}. \tag{13}$$

The above equation for the transfer function $\mathbf{T_{zd}}$ is often denoted in robust control literature as the *linear fractional operator*, $F_\ell(\mathbf{P}, \mathbf{K})$.

While converting from a state space representation to the corresponding transfer function is unique as shown in Eq. (7), the reverse is not unique. Let the *minimal realization* of **P** be **A**, **B**, **C** and **D**. Since **P** corresponds to two input vectors, **d** and **u**, and two output vectors **z** and **y**. A similar expression of Eq. (8) now is partitioned into

$$\mathbf{P} = \left[\begin{array}{c|cc} \mathbf{A} & \mathbf{B_1} & \mathbf{B_2} \\ \hline \mathbf{C_1} & \mathbf{D_{11}} & \mathbf{D_{12}} \\ \mathbf{C_2} & \mathbf{D_{21}} & \mathbf{D_{22}} \end{array}\right]. \tag{14}$$

It implies the state space form:

$$\dot{\mathbf{x}}(t) = \mathbf{A}\mathrm{x}(t) + \mathbf{B}_1\mathbf{d}(t) + \mathbf{B}_2\mathbf{u}(t), \tag{15}$$

$$\mathbf{z}(t) = \mathbf{C}_1\mathbf{x}(t) + \mathbf{D}_{11}\mathbf{d}(t) + \mathbf{D}_{12}\mathbf{u}(t) \tag{16}$$

and

$$\mathbf{y}(t) = \mathbf{C}_2\mathbf{x}(t) + \mathbf{D}_{21}\mathbf{d}(t) + \mathbf{D}_{22}\mathbf{u}(t). \tag{17}$$

The H_2 solution procedure in Doyle et al. [8] is based on the state space realization of the transfer function **P** particularly with $\mathbf{D_{11}} = \mathbf{D_{22}} = 0$.

The H_2 control has the advantage of satisfying the given robustness requirements; in terms of the linear quadratic Gaussian (LQG) stochastic control, this corresponds to a judicious and well-motivated choice of the weighting matrices of the quadratic criterion [10].

The freedom of choosing elements for **z** and frequency-dependent weighting functions make H_2 approach very flexible. In the application of H_2 control to offshore structures, it is reasonable to assume that the plant transfer function **P** is real, *rational* and *proper*. It implies that the transfer function **P** can be expressed as *rational* functions in s with *real* coefficients, and **P** is *proper* if $\mathbf{P}(\infty)$ is finite. The goal is to seek a real, rational, and proper transfer function matrix **K** to minimize the H_2 norm of the transfer matrix connecting **d** and **z**, under the constraint that internal stability be guaranteed. One must notice that the H_2 control algorithm requires the input signal vector **d** (external disturbance, sensor noise, model uncertainty) be white noise processes. However, external disturbance due to the realistic wave force acting on the offshore structure is not a white noise process. In order to meet this white noise input requirement, a *force filter* that produces desired wave force characteristics as output from a white noise input must be introduced. The wave force filter eventually will be combined with the structure as part of the "generalized" plant.

In addition to the input noise term to generate the desired wave force, other noise terms must include to account for model uncertainties and measurement errors. Model uncertainties stem from at least two sources: (i) Often the higher vibration modes of a structure are discarded in the model. Therefore, one form of uncertainty is due to neglected dynamics. (ii) The actual mass or stiffness of some element of the dynamical system always differs to some degree from the model value. This is called parametric uncertainty.

Noise terms designated to generate desired external forces should be separated from noise terms used to account for model uncertainties. Without separating these two is likely to produce an ill model. This is because when one intends to tune the weighting between model uncertainty and measurement error, it would affect the intended environmental forces as well. It is noticed that in the previous application of H_2 control by Spencer et al. [7] to seismic-induced vibration problem

and the application by Suhardjo and Kareem [6] to wave-induced vibration problem, both studies employed only one noise term to generate filtered environment forces and to account for model uncertainties. In the present study, noise terms for generating filtered wave loading and accounting for model uncertainty will be separated.

3. Problem formulation

The intention of this study is having an active mass damper (AMD) that is placed at the deck of a template offshore platform by applying H_2 control algorithm to reduce the deck motion. First, one can apply the finite element method to numerically model the fixed offshore platform as a multi-degree-of-freedom (m.d.o.f.) system. In the present study, for simplicity, the offshore structure is simplified to be a single-degree-of-freedom (s.d.o.f.) system that is governed by its first vibration mode. The simplification procedure can be based on a standard eigenanalysis to identify its first mode and corresponding modal parameters. Usually this s.d.o.f. model represents an appropriate approximation for the structural model due to the reason that typical wave-resistant offshore structures are designed to have the structural fundamental frequency much larger than the dominant wave frequency, and therefore the structural response is always dominated by the first mode. In consequence, a s.d.o.f. consideration for the structural model is adequate for vibration control purpose.

Denote the *modal* mass, stiffness, and damping associated with the simplified s.d.o.f. offshore structure to be m_1, k_1 and c_1; and the corresponding modal co-ordinate refers to the deck motion of the offshore structure, denoted by x_s. The mass, stiffness, and damping of the AMD located at the deck are denoted to be m_2, k_2 and c_2; and the displacement of the AMD is x_a. A sketch of the combined system is shown in Fig. 3, where u and p represent the active control force and the generalized (modal) wave force, respectively. Mathematically, the equations of motion for the combined system can be described by two coupled second order differential equations as

$$m_1\ddot{x}_s + c_1\dot{x}_s + k_1x_s = p - u + c_2(\dot{x}_a - \dot{x}_s) + k_2(x_a - x_s), \tag{18}$$

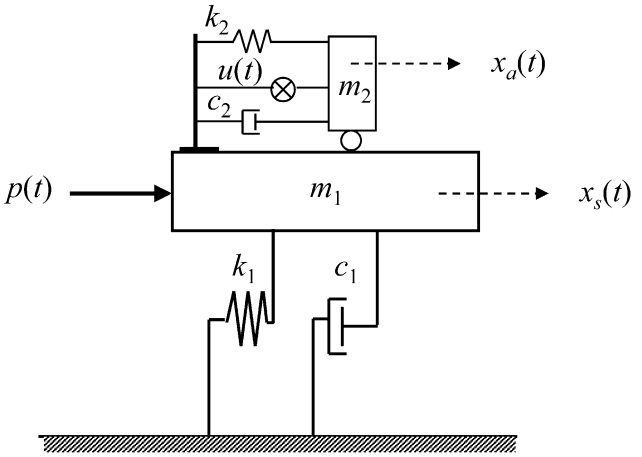

Fig. 3. An idealized two-degree-of-freedom system.

$$m_2\ddot{x}_a + c_2(\dot{x}_a - \dot{x}_s) + k_2(x_a - x_s) = u. \tag{19}$$

Letting $x = \{x_s, x_a, \dot{x}_s, \dot{x}_a\}^{\mathrm{T}}$, where superscript T stands for transpose, and using a state space representation for the combined system, one shows

$$\dot{\mathbf{x}} = \mathbf{A}\mathbf{x} + \mathbf{B}u + \mathbf{E}p, \tag{20}$$

where

$$\mathbf{A} = \begin{bmatrix} 0 & 0 & 1 & 0 \\ 0 & 0 & 0 & 1 \\ \dfrac{-k_1 - k_2}{m_1} & \dfrac{k_2}{m_1} & \dfrac{-c_1 - c_2}{m_1} & \dfrac{c_2}{m_1} \\ \dfrac{k_2}{m_2} & \dfrac{-k_2}{m_2} & \dfrac{c_2}{m_2} & \dfrac{-c_2}{m_2} \end{bmatrix}, \tag{21}$$

$$\mathbf{B} = \begin{Bmatrix} 0 \\ 0 \\ \dfrac{-1}{m_1} \\ \dfrac{1}{m_2} \end{Bmatrix} \tag{22}$$

and

$$\mathbf{E} = \begin{Bmatrix} 0 \\ 0 \\ \dfrac{1}{m_1} \\ 0 \end{Bmatrix}. \tag{23}$$

To account for model uncertainties, adding a vector noise term, $\mathbf{w}$, to Eq. (20), one obtains

$$\dot{\mathbf{x}} = \mathbf{A}\mathbf{x} + \mathbf{B}u + \mathbf{E}p + \mathbf{w}. \tag{24}$$

In the next section, the transfer function for a filter, denoted as $F(s)$, to output the generalized wave force $p(t)$ from a unit white noise process, w_1, will be developed. Based on the equation of motion given in Eq. (24) and the framework of H_2 control block diagram, one assigns the input $\mathbf{d}$ as

$$\mathbf{d} = \begin{Bmatrix} w_1 \\ \mathbf{w} \\ \mathbf{v} \end{Bmatrix}, \tag{25}$$

where $\mathbf{v}$ represents the measurement noise vector. The dimension of $\mathbf{w}$ is the number of state variables, N_s; and the dimension of $\mathbf{v}$ is the number of measurements, N_m. Elements of the white noise vector $\mathbf{w}$, as well as those of $\mathbf{v}$, could be correlated with various variances. Vectors $\mathbf{w}$ and $\mathbf{v}$ can also be expressed mathematically as linear transformations of uncorrelated unit white noise

processes as

$$\mathbf{w} = \mathbf{L}_{\mathbf{w}}\mathbf{n}_{\mathbf{w}}, \tag{26}$$

$$\mathbf{v} = \mathbf{L}_{\mathbf{v}}\mathbf{n}_{\mathbf{v}}, \tag{27}$$

where $\mathbf{n}_{\mathbf{w}}$ and $\mathbf{n}_{\mathbf{v}}$ represent uncorrelated unit white noise process vector with dimension N_s and N_m, respectively, and $\mathbf{L}_{\mathbf{w}}$ and $\mathbf{L}_{\mathbf{v}}$ are square matrices of dimensions N_s and N_m.

The regulated output $\mathbf{z}$ normally contains two components:

$$\mathbf{z} = \begin{Bmatrix} \mathbf{z}_1 \\ \mathbf{z}_2 \end{Bmatrix}, \tag{28}$$

where $\mathbf{z}_1$ is the weighted structural response and $\mathbf{z}_2$ is the weighted control force. The dimension of $\mathbf{z}_1$ and $\mathbf{z}_2$ both can be greater than one. However, in the present application, only one control force will be available. For simplicity, the weighted structural response will be chosen to be one also.

A detailed H_2 control block diagram representation of the system given in Eq. (24) is depicted in Fig. 4. In this figure, in addition to those symbols that have been defined, $\mathbf{C}_{\mathbf{y}}$ and $\mathbf{C}_{\mathbf{z}}$ are constant matrices that dictate the components of structural response comprising the measured output vector $\mathbf{y}$ and the regulated response, respectively. For a single control force and a single regulated response, W_1 and W_2 are frequency-dependent weighting functions, and α_1 and α_2 are scalar multipliers for W_1 and W_2, respectively. Increasing $\alpha_1 W_1$ in a frequency range causes the transfer function from w_1 and $\mathbf{w}$ to the weighted structural response z_1 to be minimized more. This will help improve the performance of the system at those frequencies. Increasing $\alpha_2 W_2$ in a frequency range causes the transfer function from u to the weighted control force z_2 to be minimized more. This will help limit the control forces. Increasing one of the weightings in

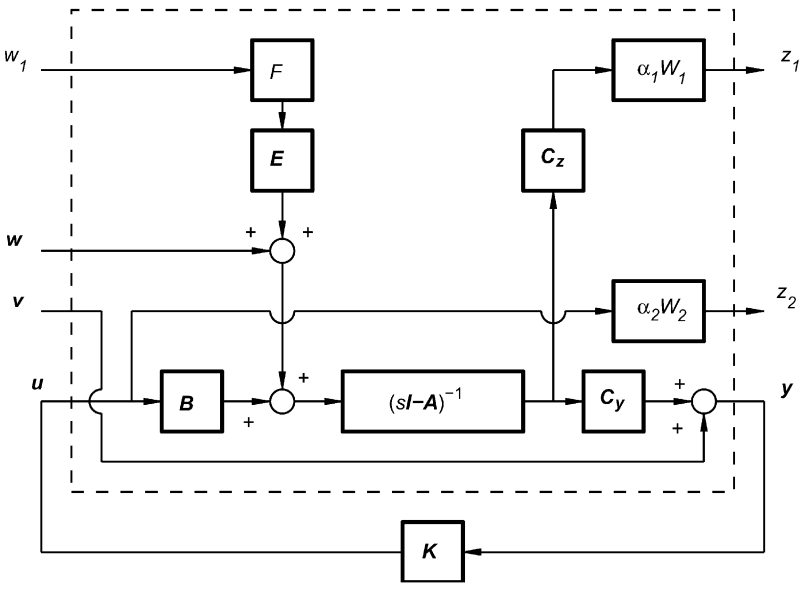

Fig. 4. H_2 control block diagram for offshore structures subjected to waves.

frequency range decreases the importance of the other weighting in that frequency range. With this set-up, the matrix **P** expressed in the form of Eq. (11) is given by

$$\mathbf{P} = \left[\begin{array}{c|c} \mathbf{P_{zd}} & \mathbf{P_{zu}} \\ \hline \mathbf{P_{yd}} & \mathbf{P_{yu}} \end{array}\right] = \left[\begin{array}{ccc|c} P_{z_1w_1} & \mathbf{P}_{z_1\mathrm{w}} & \mathbf{P}_{z_1\mathrm{v}} & P_{z_1u} \\ P_{z_2w_1} & \mathbf{P}_{z_2\mathrm{w}} & \mathbf{P}_{z_2\mathrm{v}} & P_{z_2u} \\ \hline \mathbf{P}_{\mathbf{y}w_1} & \mathbf{P}_{\mathbf{yw}} & \mathbf{P}_{\mathrm{yv}} & \mathbf{P}_{yu} \end{array}\right] \tag{29}$$

in which each component can be obtained simply by following an appropriate path of Fig. 4. For instance, the way to obtain $P_{z_1w_1}$ is by tracing the path from w_1 to z_1. One needs to pre-multiply all passing blocks from w_1 to z_1 to obtain: $P_{z_1w_1} = \alpha_1 W_1 \mathbf{C_z}(s\mathbf{I} - \mathbf{A})^{-1}\mathbf{E}F$. Following a similar procedure, one obtains the complete information of **P** as

$$\mathbf{P} = \left[\begin{array}{ccc|c} \alpha_1 W_1 \mathbf{C_z} \mathrm{GE}F & \alpha_1 W_1 \mathbf{C_z G} & 0 & \alpha_1 W_1 \mathbf{C_z GB} \\ 0 & 0 & 0 & \alpha_2 W_2 \\ \hline \mathbf{C_y GE}F & \mathbf{C_y G} & \mathrm{I} & \mathbf{C_y GB} \end{array}\right], \tag{30}$$

where $\mathbf{G} = (s\mathbf{I}—\mathrm{A})^{-1}$.

4. Generalized wave force filter

It is assumed that the wave elevation is a zero-mean, stationary, Gaussian random process, fully characterized by its wave spectrum, $S_\eta(\omega)$, i.e., *the power spectral density* function (psd) of the wave elevation, $\eta(t)$. As mentioned previously, applying the H_2 control strategy to offshore structure under such wave environment requires the design of a wave force filter. In the present study, the control is on the first mode of the offshore structure. In consequence, the filter design, given the input being a unit white noise process, should intend to get the output process that has its psd approximated to the psd of the "generalized" wave force associated with the first mode, $S_p(\omega)$. Three steps are involved in the development of the wave force filter: (i) One needs to know how to numerically calculate the $S_p(\omega)$ from a given $S_\eta(\omega)$. (ii) Once the numerical result for $S_p(\omega)$ is obtained, it is required to approximate the numerical result by a *rational* form. (iii) Finally, a *spectral factorization* must be performed on the rational psd to obtain a rational transfer function that represents the filter [11,12].

The generalized wave force corresponding to the first mode of the structure can be expressed as

$$p(t) = \int_0^d f(z,t)\phi(z)\,\mathrm{d}z, \tag{31}$$

where z is the vertical co-ordinate with the origin at the sea floor, d the water depth, $\phi(z)$ the shape function corresponding to the first mode, and $f(z,t)$ denotes the physical horizontal wave force per unit length along the cylindrical structural members that is usually estimated based on the Morison equation

$$f(z,t) = K_m\dot{v}(z,t) + K_d v(z,t)|v(z,t)|, \tag{32}$$

where $K_m = C_m\rho\pi D^2/4, K_d = \frac{1}{2}C_d\rho D, v(z,t)$ and $\dot{v}(z,t)$ are the water particle velocity and acceleration, respectively, D the diameter of the cylindrical structure, ρ fluid density, and C_m and C_d the dimensionless inertia and drag coefficients, respectively [14,15].

Following the linear wave theory, one can derive the water particle velocity, for the wave elevation with wave frequency ω, at location z related to $\eta(t)$ as

$$v(z,t) = \omega \frac{\cosh(kz)}{\sinh(kd)} \eta(t), \tag{33}$$

where k is the wave number that can be determined from the linear dispersion relationship:

$$\omega^2 = gk \tanh(kd), \tag{34}$$

where g is the gravity constant. Alternatively, one can also write Eq. (33) as

$$v(z,t) = T_{v\eta}(\omega, z)\eta(t), \tag{35}$$

where

$$T_{v\eta}(\omega, z) = \omega \frac{\cosh(kz)}{\sinh(kd)} \tag{36}$$

stands for the *complex frequency response* (CFR) function from η to v. The CFR function is related to the corresponding *transfer function* simply by the variable change $s = \mathrm{j}\omega$, where $\mathrm{j} = \sqrt{-1}$.

Similarly, applying linear wave theory, one obtains

$$\dot{v}(z,t) = T_{\dot{v}\eta}(\omega, z)\eta(t), \tag{37}$$

where the CFR function from η to $\dot{v}$ is written as

$$T_{\dot{v}\eta}(\omega, z) = -\mathrm{j}\omega^2 \frac{\cosh(kz)}{\sinh(kd)}. \tag{38}$$

As implied in Eqs. (36) and (38), the horizontal velocity and wave elevation are in phase. However, the horizontal acceleration and elevation are 90° out-of-phase.

To analytically obtain the CFR function from, η to f is difficult due to the non-linear drag term in Eq. (32). For this reason, a linearized Morison equation is commonly used [15]:

$$f(z,t) = K_m \dot{v}(z,t) + K_d \sqrt{\frac{8}{\pi}} \sigma_v(z) v(z,t), \tag{39}$$

where $\sigma_v(z)$ is the standard deviation of the velocity at location z that can be obtained as

$$\sigma_v(z) = \left[\int_0^\omega |T_{v\eta}(\omega, z)|^2 S_\eta(\omega)\, \mathrm{d}\omega \right]^{1/2}. \tag{40}$$

Substituting Eqs. (35), (37) and (39) into Eq. (31) yields

$$p(t) = T_{p\eta}(\omega)\eta(t), \tag{41}$$

where

$$T_{p\eta}(\omega) = \int_0^d \left[K_i T_{\dot{v}\eta}(\omega, z) + K_d \sqrt{\frac{8}{\pi}} \sigma_v(z) T_{v\eta}(\omega, z) \right] \phi(z)\, \mathrm{d}z. \tag{42}$$

Note that the calculation for the CFR function $T_{p\eta}(\omega)$ involves two one-dimensional numerical integrations, Eqs. (40) and (42). Given the psd of wave elevation, $S_\eta(\omega)$, and the CFR function

from η to p, $T_{p\eta}(\omega)$, one readily calculates the psd for the generalized wave force as

$$S_\eta(\omega) = |T_{p\eta}(\omega)|^2 S_\eta(\omega). \tag{43}$$

The generalized wave force filter design is based on two requirements: (i) the input is a unit white noise process, ω_1, and (ii) the psd of the output, denoted as $\hat{S}_p(\omega)$, must be as close to $S_p(\omega)$, given in Eq. (43), as possible. Theoretically, one can express $\hat{S}_p(\omega)$ to be

$$\hat{S}_p(\omega) = 1 \cdot |T_{p\omega_1}(\omega)|^2 = T_{p\omega_1}(\mathrm{i}\omega) \cdot T_{p\omega_1}(-\mathrm{i}\omega), \tag{44}$$

where $T_{p\omega_1}(\omega)$ is the CRF function from ω_1 to p. The above equation can also be written in the s-domain as

$$\hat{S}_p(s) = T_{p\omega_1}(s) T_{p\omega_1}(-s). \tag{45}$$

Now, $T_{p\omega_1}(s)$ is interpreted as the transfer function from ω_1 to p.

If the spectral function $\hat{S}_p(s)$ can be written in a rational spectral form, i.e., as a ratio of polynomials in s^2:

$$\hat{S}_p(s) = \frac{b_0 s^{2m} + b_1 s^{2(m-1)} + \cdots + b_{m-1} s^2 + b_m}{a_0 s^{2n} + a_1 s^{2(n-1)} + \cdots + a_{n-1} s^2 + a_n}, \quad n \geqslant m+1, \tag{46}$$

then the *spectral factorization* can be used to write the function in the form:

$$\hat{S}_p(s) = \frac{c(s)}{d(s)} \cdot \frac{c(-s)}{d(-s)}, \tag{47}$$

where $c(s)/d(s)$ has all its poles and zeros in the left half-plane and $c(-s)/d(-s)$ has mirror-image poles and zeros in the right half-plane. The order of the denominator n being at least one greater than the numerator m is necessary in order for the output process to have a finite variance. A direct comparison of Eqs. (44) and (47) suggests [12]

$$T_{p\omega_1}(s) = \frac{c(s)}{d(s)}. \tag{48}$$

In numerical implementation, a specific form for $\hat{S}_p(s)$ in Eq. (46) must be chosen a priori; and the corresponding numerator and denominator coefficients can be determined by a standard least-squares approach when numerical result of $\hat{S}_p(\omega)$ from Eq. (43) becomes available.

5. Numerical example

The structure adopted in the numerical study is an offshore platform of length 249 m (L) placed in 218 m (d) of water. The structural configuration consists of a template structure with four main legs. After applying the finite element method to numerically model the fixed offshore platform as a MDOF system, the offshore structure is simplified to be a s.d.o.f. system governed by its first vibration mode. The *generalized* mass associated with the simplified s.d.o.f. offshore structure is obtained to be $m_1 = 7\,825\,307$ kg. The corresponding vibration frequency is 2.048 rad/s that amounts to a structural period 3.07 s. It is assumed the structural damping ratio for the first mode is 2%. The mass of the AMD located at the deck is taken to be 1% of first modal mass of structure, i.e., $m_2 = 78\,253$ kg. The stiffness and damping of the AMD are determined based on an

optimal design for a tuned mass damper (TMD) where the vibration period and damping ratio of the TMD are taken to be 3.13 s (98% of the first modal frequency of the structure) and 20%, respectively [13].

The random wave condition is assumed to be Gaussian and stationary, characterized by a JONSWAP spectrum [14,15]:

$$\hat{S}_p(\omega) = \left(\frac{5H_s^2}{16\omega_0}\right)\left(\frac{\omega_0}{\omega}\right)^5 \exp[-1.25(\omega/\omega_0)^{-4}]\gamma^{\beta}, \tag{49}$$

where H_s is the significant wave height, ω_0 the dominant (peak) wave frequency, γ the peakedness coefficient being taken to be 3.3, and $\beta = \exp[-(\omega-\omega_0)^2/(2\tau^2\omega_0^2)]$ in which $\tau = 0.07$ for $\omega \leqslant \omega_0$ and $\tau = 0.09$ for $\omega \geqslant \omega_0$. Unless stated otherwise, the numerical study below is based on $H_s = 7$ m and $\omega_0 = 0.79$ rad/s (i.e., dominant wave period = 8 s).

The standard deviation of the horizontal water particle velocity decays exponentially with depth. While applying Eq. (31) to calculate the generalized wave force corresponding to the first mode of the structure, one approximates the shape function as a function of z:

$$\phi(z) = 1 - \cos\left(\frac{\pi z}{2L}\right), \quad 0 \leqslant z \leqslant L. \tag{50}$$

Furthermore, following equations (42) and (43), one can calculate the psd for the generalized wave force. Taking $C_m = 1.5$, $C_d = 1.0$ and $D = 1.83$ m, one obtains the numerical result of the psd function of the generalized wave force acting on the structure, $S_p(\omega)$, shown as the broken line in Fig. 5.

In order to obtain a rational form for the transfer function $T_{p\omega_1}(s)$ associated with the generalized wave force filter, one needs first to obtain a rational form for the numerical psd $S_p(\omega)$. By referring to Spanos [16], the mathematical model for the rational psd $\hat{S}_p(\omega)$ is chosen to be

$$\hat{S}_p(\omega) = |T_{p\omega_1}(\omega)|^2 = \frac{b\left(\frac{\omega}{\omega_0}\right)}{\left(\frac{\omega}{\omega_0}\right)^8 + a_1\left(\frac{\omega}{\omega_0}\right)^6 + a_2\left(\frac{\omega}{\omega_0}\right)^4 + a_3\left(\frac{\omega}{\omega_0}\right)^2 + a_4}, \tag{51}$$

where ω_0 is the peak frequency corresponding to the JONSWAP wave spectrum. Coefficients a_1, a_2, a_3, a_4 and b are determined based on an ordinary least-squares approach. The solid line shown in Fig. 5 is the obtained $\hat{S}_p(\omega)$. It suggests that the estimated analytical spectrum is in good agreement with the numerical spectrum.

In turn, expressed in the s-domain, the corresponding $\hat{S}_p(s)$ is written as

$$\hat{S}_p(s) = \frac{b^* s^4}{s^8 + a_1^* s^6 + a_2^* s^4 + a_3^* s^2 + a_4^*}, \tag{52}$$

where $a_1^* = -a_1\omega_0^2, a_2^* = a_2\omega_0^4, a_3^* = -a_3\omega_0^6, a_4^* = a_4\omega_0^8$, and $b^* = b\omega_0^4$. Once all coefficients of Eq. (52) are known, the transfer function for the generalized wave force filter, denoted as F in the block diagram shown in Fig. 4, can be obtained by performing the spectral factorization of Eq. (52).

While applying H_2 optimization control, choosing the weighting functions is crucial for obtaining meaningful engineering results. In general, a direct application of the H_2 optimization

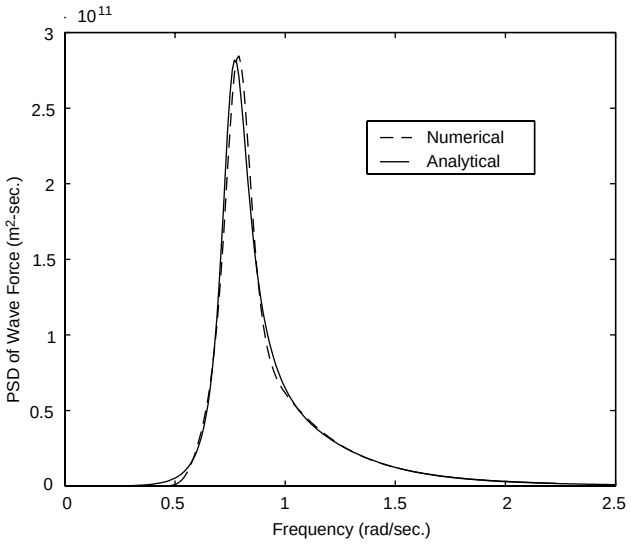

Fig. 5. Numerical and analytical psd functions for generalized wave force.

seeks to minimizing the H_2 norm over all frequencies without placing more emphasis or penalty on certain frequency ranges. For the control model used in this study, frequency-dependent weighting functions W_1 and W_2 are employed to reflect the cost (penalty) functions for the deck motion and control force, respectively. In practical implementation of the controller, control action at higher frequencies is usually of little benefit and may in fact be detrimental to the performance of the system due to *spill-over* effects. It is usually intended to reduce the structural response in the frequency range where the structure is sensitive to disturbance, i.e., at low frequencies. At high frequencies where the structure is often not sensitive to disturbance, It is desire to "roll off" or lower the control because the control is not effective. Hence the choice for W_1 should have a large magnitude at low frequencies and roll off at high frequencies. For the choice of W_2, it is intended not to inject high frequency control forces into the system, partially due to the limitation of the control hardware. Therefore, the weighting function should have high weighting on high frequency and low weighting on low frequency. In the present numerical study, the weighting functions are given as

$$W_1 = \frac{4}{s+4} \tag{53}$$

and

$$W_2 = \frac{s+0.1}{s+4}. \tag{54}$$

Magnitudes of the functions W_1 and W_2 versus frequency are shown in Fig. 6. As can be seen, the weighting function associated with deck motion is highest at the low frequencies and drops with increasing frequency. The weighting function associated with control force is very low at the low frequencies and increases with higher frequencies. This provides a system that will give the most control at low frequencies, and will tend to ignore motion at the higher frequencies. The

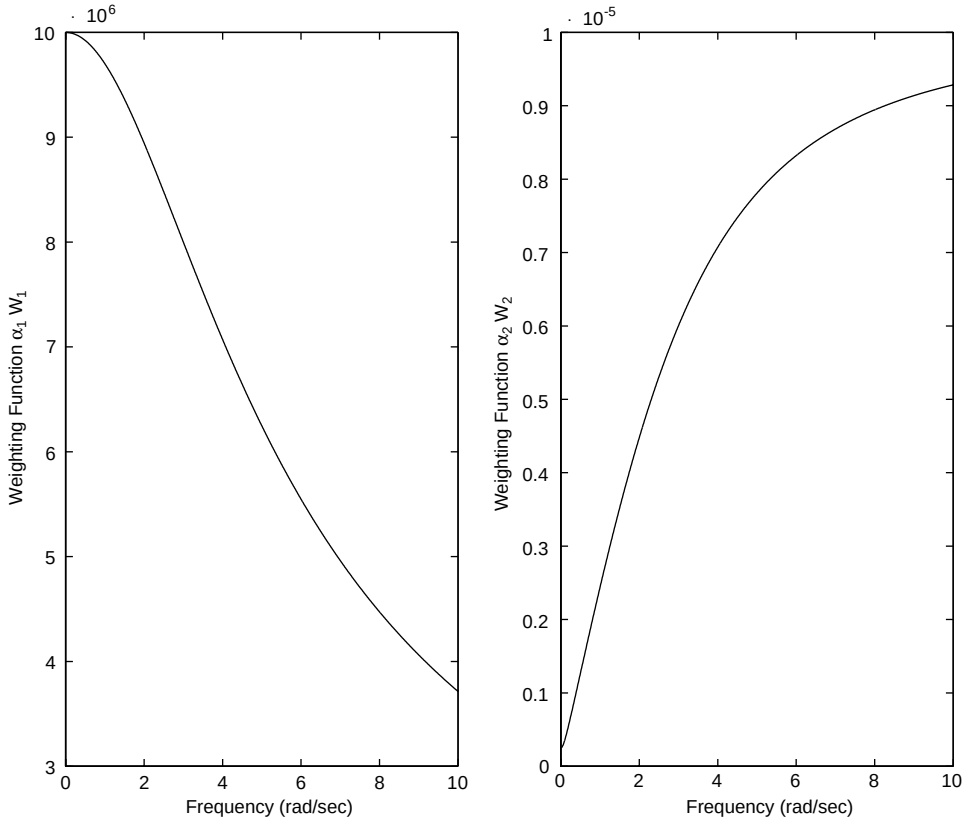

Fig. 6. Weighting functions versus frequency.

coefficients α_1 and α_2 are constant quantities that intend to bring the scale, and unit as well, of the deck motion and control force to be comparable and consistent.

The noise level associated with the measurements and the uncertainty associated with the plant model ideally should be determined based on the best engineering judgment prior to applying the control algorithm. However, it is not unusual to tune the relative noise level during the implementation time. It is also realized that the performance of the H_2 control is highly sensitive to the selection of noise levels.

Shown in Fig. 7 is an example of the results about magnitudes of the transfer function from unit white noise to weighted deck motion $T_{z_1\omega_1}$ for cases: (i) with no control, (ii) with a passive TMD, and (iii) with an AMD controlled by H_2 algorithm. It basically demonstrates that installing a TMD with its frequency tuned near to the fundamental structural frequency enables to reduce the deck motion of the offshore structure, only effective in the frequency range near to the fundamental structural frequency, and that properly applying an H_2 control algorithm together with an AMD can significantly reduce the deck vibration for a wide frequency range, covering ranges of significance to both the ocean wave and the offshore structure.

The numerical comparison of standard deviations of deck motion, denoted as σ_{x1}, for the above three control cases are given in Table 1. The standard deviation of the deck motion with a TMD is

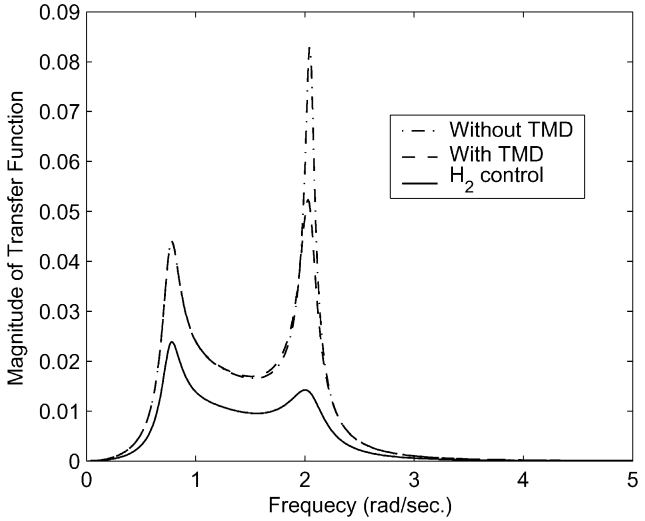

Fig. 7. Magnitude of the transfer functions from unit white noise w_1 to the weighted deck motion z_1.

Table 1
Standard deviations of deck motion and control force ($H_s = 6\,\text{m}$, $\omega_o = 0.78\,\text{rad/s}$)

	σ_{x1} (cm)	σ_u (kN)
No control	1.71	—
TMD control	1.36	—
H_2 control	0.86	661.7

calculated to be 2.77 cm; and that with H_2 control is 1.69 cm. This represents a reduction of approximately 50.01%. In this table, σ_u represents the standard deviation associated with the required active control force by H_2 control algorithm.

6. Concluding remarks

Similar to the study by Suhardjo and Kareem [6], this article has been devoted to developing a proper procedure on applying H_2 control algorithm for controlling the lateral vibration of a jacket-type offshore platform by using an AMD. A number of improvements in problem formulation, wave force filter design, and control algorithm implementation are made at various stages. Unlike the study by Suhardjo and Kareem [6], which adopted a shear building model, the present paper models a realistic offshore platform by using a finite element approach. In implementing H_2 algorithm, the vibration control is conducted in the domain of modal (generalized) co-ordinates. This modal approach greatly simplifies the wave force filter design, in which the "generalized" wave force is determined based on an analytical approximation of the

mode shape function, together with the physical wave loading being calculated from a linearized Morison equation. Another significant improvement over previous studies is on the issue about the separation of white noise terms corresponding to wave force filter and dynamic model uncertainty. The introduction of a separated noise term is important to meet the underlying principles associated with H_2 control algorithm. With this change, it allows the algorithm to freely vary the weighting of error between measurement and dynamic model of the system, but keeps the design wave force "size" intact. In addition, the present paper also numerically demonstrated the effectiveness of H_2 active control. As expected, it significantly outperforms the corresponding passive control that uses a TMD.

Acknowledgements

This research is partially supported by National Natural Science Foundation of China, No.50179014. The support is gratefully appreciated.

References

[1] T.T. Soong, Active Structural Control: Theory & Practice, Longman Scientific and Technical, England, 1990.
[2] G.W. Housner, et al., Structural control: past present and future, American Society of Civil Engineers Journal of Engineering Mechanics 123 (9) (1997) 897–971.
[3] S. Sirlin, et al., Active control of floating structures, American Society of Civil Engineers Journal of Engineering Mechanics 112 (9) (1986) 947–965.
[4] K. Yoshida, H. Suzuki, N. Oka, Control of dynamic responses of towerlike offshore structures in waves, Transactions of the American Society of Mechanical Engineers 112 (1990) 14–20.
[5] M. Abdel-Rohman, Structural control of a steel jacket platform, Structural Engineering and Mechanics 4 (2) (1996) 125–138.
[6] J. Suhardjo, A. Kareem, Structural control of offshore platforms, Proceedings of the Seventh ISOPE, Honolulu, 1997, pp. 416–424.
[7] B.F. Spencer, J. Suhardjo, M.K. Sain, Frequency domain optimal control strategies for aseismic protection, American Society of Civil Engineers Journal of Engineering Mechanics 120 (1) (1994) 135–159.
[8] J.C. Doyle, K. Glover, P. Khargonekar, B. Francis, State-space solutions to standard H_2 and H_∞ control problems, IEEE Transactions on Automatic Control 34 (1989) 831–874.
[9] S.P. Boyd, C.H. Barrantt, Linear Controller Design: Limits of Performance, Prentice-Hall, Englewood Cliffs, NJ, 1991.
[10] V. Sima, Algorithms for Linear-quadratic Optimization, Marcel Dekker, New York, 1996.
[11] B.D.O. Anderson, An algebraic solution to the spectral factorization problem, IEEE Transactions on Automatic Control AC-12 (1967) 410–414.
[12] R.G. Brown, P.Y.C. Hwang, Introduction to Random Signals and Kalman Filtering, 2nd Edition, Wiley, New York, 1992.
[13] H. Li, S.L.J. Hu, Tuned mass damper design for optimally minimizing fatigue damage, American Society of Civil Engineers Journal of Engineering Mechanics 178 (6) (2002) 703–708.
[14] S.K. Chakrabarti, Hydrodynamics of Offshore Structures, Springer, Berlin, 1987.
[15] T. Sarpkaya, M. Isaacson, Mechanics of Wave Forces on Offshore Structures, Van Nostrand Reihhold, New York, 1981.
[16] P.T.D. Spanos, Filter approaches to wave kinematics approximation, Applied Ocean Research 8 (1) (1986) 2–7.